Root-pore interactions, the underestimated driver for rhizosphere structure and rhizosheath development

Maik Lucas[1*], Andrey Guber[2], Alexandra Kravchenko[2]

1 Institute of Ecology, Chair of Soil Science, Technical University Berlin, 10587 Berlin, Germany

2 DOE Great Lakes Bioenergy Research Center, Department of Plant, Soil and Microbial Sciences, Michigan State University, East Lansing, MI, 48824, USA

*Corresponding author

E-mail address: lucas@tu-berlin.de

• Physical characteristics of rhizosphere are crucial for plant performance; and analyses of rhizosheath, i.e. root-adhering soil, is a common tool in rhizosphere studies. Yet, despite numerous efforts, processes that lead to formation of rhizosphere porosity gradients, as well as their relationships with rhizosheath, remain poorly understood.

• We used X-ray computed micro-tomography (µCT) to examine rhizosphere porosity and to distinguish between the effect of direct root-induced changes vs. that of preferential root growth patterns on observed rhizosphere macroporosity gradients. We also utilized ^{14}C labeling to evaluate rhizosheath in relation to rhizosphere macroporosity and rhizodeposition. The experiments were conducted in intact soil with inherent structure preserved and in sieved structureless soil.

• Rhizosphere macroporosity was found to be largely the outcome of root growth preferences, while root-induced changes occurred at <0.1 mm distances from the root surface and primarily in sieved soils. Rhizosheath formation was linked to the roots actively compacting their surrounding and releasing carbon in it, while there was no link between destructively-sampled rhizosheath and intactly µCT-observed rhizosphere.

• The findings suggest that root-soil interactions, rather than root-induced changes, drive rhizosphere porosity. Rhizosheath development compensates for low soil-root contact, however, traditionally sampled rhizosheath is not representative of the actual rhizosphere.

Key words: Rhizosheath, X-ray CT, root-pore interactions, macroporosity gradients, root growth preferences, rhizosphere self-organization

1 Introduction

Rhizosphere, the narrow zone of soil directly surrounding plant roots, is one of the most dynamic regions within the soil that frequently undergoes rapid and significant alterations in its physical, chemical, and biological properties (Hinsinger *et al.*, 2009). Modifications in soil structure, i.e. arrangement of soil solids and pores, are arguably the most prominent and impactful of such root-induced changes. The rhizosphere is the bottleneck through which water and nutrients must flow when they are either released or taken up by the plant root, and these fluxes occur via soil pores. Thus, structural changes in characteristics of pore and solid components forming the rhizosphere have a direct impact on water flow, nutrient cycling, and carbon storage (Aravena *et al.*, 2011; van Veelen *et al.*, 2019; Landl *et al.*, 2021; Pankievicz *et al.*, 2022; Lucas *et al.*, 2023).

Rhizosphere pore structure is often reported to differ significantly from that of bulk soil (Helliwell *et al.*, 2019; Koebernick *et al.*, 2019; Lucas *et al.*, 2019), i.e., the soil not influenced by the roots. However, the findings are often contradictory. For example, several works that used X-ray computed tomography (X-ray µCT), currently the most advanced approach for *in situ* visualization of plant roots and their contact with the soil, reported reduction in soil macroporosity within the rhizosphere (Feeney *et al.*, 2006; Helliwell *et al.*, 2017, 2019; Rabbi *et al.*, 2018a,b; Zhang *et al.*, 2020), while many others noted the increases (Bruand *et al.*, 1996; Vollsnes *et al.*, 2010; Lucas *et al.*, 2019). Such discrepancies substantially limit the progress in understanding and modeling plant-soil interactions (van Veelen *et al.*, 2019; Landl *et al.*, 2021; Schnepf *et al.*, 2022).

We surmise that the reported contradictions in porosity gradients around the roots result from simultaneous contributions of two disparate mechanisms: 1) direct root-induced changes and 2) indirect effects of root growth preferences. Direct changes take place when roots compress the rhizosphere soil while moving into and growing through relatively small pores, reducing the rhizosphere macroporosity (Dexter, 1987). Later, the initial reduction can be somewhat abated due to structural changes generated by combined impacts of rhizodeposition, enhanced wetting/drying cycles in vicinity of the roots (Koebernick *et al.*, 2018), root shrinkage during soil drying, and the "surface-wall effect"

(Carminati *et al.*, 2013; Koebernick *et al.*, 2019). The latter refers to the packing of round-shaped soil particles against the growing root, which can increase macroporosity at the root surface (Koebernick *et al.*, 2019).

The indirect outcomes arise from roots often preferring to grow into areas of low penetration resistance, such as large macropores (White & Kirkegaard, 2010; Lucas *et al.*, 2019, 2022). In such cases, root growth might have a minimal impact on the surrounding soil structure. However, the macropores themselves often already contain greater proportions of smaller pores in their vicinity. Roots populating such macropores will have a highly porous rhizosphere, due to existing soil pore structure and root growth preferences within it, rather than being an outcome of active soil modifications by the roots.

We argue that root growth preferences play a more critical role in shaping the rhizosphere's pore structure than direct root impacts, making the initial pore structure the primary factor influencing the rhizosphere's physical properties. Notably, all of the past experiments focusing on rhizosphere properties were conducted in artificially structured, e.g., sieved or mixed, soils. Such soil mixtures may not fully capture the complex interactions between roots and soil structure in natural, i.e., intact soil, environments. The intact soil is often abounded with large cracks of non-biological origin, biopores, and channels previously created by roots or living organisms (Lucas *et al.*, 2023; Vogel *et al.*, 2024), which make it a substantial experimental challenge to identify new roots and quantify their rhizosphere macroporosity. Since both root-induced changes and root growth preferences may lead to similar variations in rhizosphere macroporosity, it is challenging to separate the contributions of these two processes. Distinguishing between them, however, is crucial for modeling and predicting the effects of roots on soil pore structure and for developing process-based approaches to improving rhizosphere properties.

The structure of the rhizosphere soil is also represented by its solid components, e.g., by sizes and volumes of soil particles within it. That is often investigated in a form of a rhizosheath, which is currently operationally defined as all soil adhering to the roots and

which is considered as a practical way to sample and analyze the rhizosphere soil (Hallett *et al.*, 2022). Rhizosheath formation and soil aggregation within it are influenced by a variety of factors, including root mucilage, root hairs, and wetting-drying cycles (Watt *et al.*, 1994; Aslam *et al.*, 2022; Cheraghi *et al.*, 2023; Mo *et al.*, 2023)[1]. As part of the rhizosphere, rhizosheath soil is critical for nutrient acquisition and water retention, serving as a protective layer that increases root surface area suitable for performing these functions (Hallett *et al.*, 2022; Cheraghi *et al.*, 2023; Mo *et al.*, 2023; Mueller *et al.*, 2024). Rhizosheaths are therefore thought to buffer plants against abiotic stress, such as drought, by preventing air gaps around roots and maintaining optimal soil moisture levels (Hallett et al., 2022). While root-adhering soil represents just a fraction of the entire rhizosphere, it is commonly regarded as representative of the rhizosphere (Pang *et al.*, 2017). However, despite extensive research on rhizosheath formation, the relationship between the rhizosheath and the overall rhizosphere remains unclear, leaving the question of whether root-attached soil accurately reflects the broader rhizosphere properties unanswered.

This study has two interconnected goals: (i) to quantify the contributions of the two mechanisms defining rhizosphere pore structure, i.e., root-induced changes and inherent root growth preferences; and (ii) to investigate relationships between these two mechanisms and rhizosheath development, specifically focusing on the role of heterogeneity in soil pore structure and plant growth preferences on its formation. To achieve these goals, we reanalyzed previously published data (Lucas *et al.*, 2023), which involved Switchgrass (Panicum virgatum L.) and Black-Eyed-Susan (Rudbeckia hirta L.) grown in four types of ingrowth cores: intact and sieved cores from switchgrass and prairie systems. For the first time, we will differentiate mechanisms defining rhizosphere macropore structure by analyzing images from repeated X-ray µCT imaging (before and after plant growth) and link rhizosheath measurements via conventional soil sampling with

[1] Note that originally, the term rhizosheath was introduced for desert soils and referred to a distinct, sheath-like soil layer, created by rhizodeposits gluing soil particles together during drying and bound to the root surface (Price, 1911; Watt *et al.*, 1994; Pang *et al.*, 2017; Ndour *et al.*, 2020; Mo *et al.*, 2023).

rhizosphere soil matrix determined via X-ray µCT. The rhizosphere soil matrix is used here as a proxy for rhizosphere soil mass and calculated by excluding image derived macropores from the denser soil volume of the rhizosphere.

We hypothesize, first, that in intact soils, the contribution of root-induced changes to formation of rhizosphere pore structure will be minimal as roots will primarily reuse existing macropores, with macroporosity gradients largely driven by inherent root growth preferences. As a result, the changes in the total macropororsity (pores > 0.04 mm Ø) in intact soil cores will be less than in those composed from sieved soils. Second, increased root-induced rhizosphere compaction and greater amounts of root-derived carbon within the rhizosphere will enhance soil adhesion to the roots, promoting rhizosheath development. Third, the greater the overall volume of the rhizosphere soil matrix, the greater will be the rhizosheath mass, revealing that the rhizosheath is indeed a representative sample of the rhizosphere.

2 Methods

2.1 Experimental design and ^{14}C labeling

This study analyzed images from an experiment reported by Lucas et al. (2023), which provides detailed information about the experimental settings and plant growth conditions. Briefly, a split pot experiment was conducted using ingrowth cores (5 cm diameter) with different soil origins and pore structures (Fig. 1A). The cores were collected from the DOE-Great Lakes Bioenergy Research Center's (GLBRC) Marginal Land Experiment (MLE) site, established in 2013 in Oregon, Wisconsin. The plots sampled for this study had a long-term (7 years) history of disparate vegetation, namely, monoculture switchgrass (*Panicum virgatum* variety Cave-in-Rock) and restored prairie (an 18-species mix), the plant systems known for their roles in developing contrasting pore structures (Kravchenko *et al.*, 2019; Li *et al.*, 2024). A total of 60 intact cores were taken from the replicated experimental plots of both plant systems, with half of the cores kept intact and the rest sieved and repacked to the same bulk density. To ensure that the intact and sieved cores differed from each other only in terms of pore structure, the sieved soil was packed to the same bulk density as the intact cores and all >2 mm inclusions, such as stones and large

root residues were incorporated back into the sieved soil prior to packing. We then placed four ingrowth cores into each of twelve pots (15 cm diameter, 20 cm height), with six replicated pots per plant species. Pregerminated plants of *P. virgatum* and *R. hirta* were transplanted into the pots (one plant per pot) and grown for 48 days in a controlled growth chamber. Additionally, three unplanted control pots were prepared and maintained under the same conditions as the planted pots.

Each core was subjected to X-ray µCT before and after the plant growth experiment. Details on X-ray µCT scanning and image processing are reported in Lucas et al. (2023) and presented in the Appendix (Method S1). Double scanning enabled us to describe root growth patterns as a function of soil origin and structure as well as to quantify the proportions of roots growing into soil regions with disparate pore structures. Table 1 summarizes plant growth parameters as well as the share of roots grown into soil regions with different pore structures, namely, into soil dominated by < 0.04 mm Ø pores (soil matrix), into macropores (> 0.04 mm Ø), and into biopores (as determined in Lucas et al 2023). The latter include all macropores of biological origin and thus of cylindrical shape.

The plants were labelled with ^{14}C-CO_2 according to Santiago et al. (2021) with a constant flow from a pressurized $^{14}CO_2$ tank, which ensured a concentration of 420 µmol mol^{-1} of labelled CO_2 in the chamber. To ensure a distribution of ^{14}C in the whole root system (Pausch & Kuzyakov, 2011) as well as sufficient amounts of detectable ^{14}C in the rhizosphere, the plants were labelled at 11th and 3rd day before harvest under the same environmental conditions as set in the growth chamber.

2.2 Analyses of rhizosheath and rhizodeposition

During the harvest, the pots were disassembled, and the ingrowth cores were removed. The cores were cut open, and roots were meticulously extracted from the soil using tweezers. The roots were gently shaken to remove loosely adhering soil, and the root-adhering soil, termed rhizosheath, was carefully removed with small brushes. The rhizosheath soil was then oven-dried at 60°C to determine its dry weight. Subsequently, the dried rhizosheath soil was combusted in an oxidizer (PerkinElmer®, Boston, MA,

Model A307), and the released $^{14}CO_2$ was trapped in 20 ml of scintillation cocktail (Carbo-Sorb E:Permafluor® E+, 1:1 [v/v], PerkinElmer, Groningen, Netherlands). The radioactivity of the rhizosheath was measured using a liquid scintillation counter (PerkinElmer® Tri-Carb 4910TR, Waltham, MA).

2.3 Image analysis

Pore size distribution (PSD) were calculated from the segmented pore/solid binary images. PSD was determined in Fiji using the local thickness method (Hildebrand & Rüegsegger, 1997). Images from after the experiment contained both, newly grown roots and old roots from the field. To differentiate new from old roots, all roots were segmented in images before and after the experiment and subtracted from each other to create a mask of roots grown during the experiment. Root growth preferences were analyzed by using this mask on the segmented image from before the experiment (labeled by macropores, matrix, biopores, and roots, Fig. S1) to calculate the volume percentage of each structure encountered by the root.

Rhizosphere macroporosity gradients were calculated using the Euclidean Distance Transform (EDT) in Fiji, following Lucas et al. (2019). Besides the overall macroporosity (pores > 0.04 mm), we focused on the formation of narrow pores (0.04-0.15 mm). The later have been shown to provide ideal conditions for microbial activity (Ruamps *et al.*, 2013; Kravchenko *et al.*, 2019; Li *et al.*, 2024). The EDT computes the Euclidean distance to the nearest root for every voxel in the 3D images. The EDT of the newly developed roots was combined with the binary pore images and the PSD images from before and after plant growth to calculate gradients of all macropores and narrow pores around the roots, or more precisely their local percentage to the total local soil volume. Note that in this analysis biopores are included, being only a subset (in shape) of macropores of different sizes. The resulting pore gradients from before and after root growth were used to differentiate between changes directly induced by the roots, i.e., root-driven changes, and macroporosity gradients resulting from inherent root growth preferences (Fig. 1B). The changes in macroporosity gradients due to root activity were calculated by subtracting the local macroporosity before root growth from that after root growth; these will be

referred to as 'root-induced changes'. The macroporosity gradients resulting from root growth preferences were calculated by subtracting the mean total macroporosity of the sample from the local macroporosity at each distance from the root surface and will be referred to as the 'root *growth preference effect*'. These values were calculated for two distance increments: 0.0-0.1 mm and 0.1-0.3 mm from the roots. The selection of the distance increments was dictated by the following considerations: The 0.0-0.1 mm distance is typically associated with root shrinkage and soil surface wall effect, i.e. rearrangement of soil particles near root surface, while the 0.1-0.3 distance is the zone that in previous experiments was often found to be compressed by root growth (Koebernick *et al.*, 2019; Lucas *et al.*, 2019; Phalempin *et al.*, 2021). The µCT derived volume of the soil matrix in the rhizosphere, calculated as: 1- the local macroporosity within 0.0-0.3 mm distance from the root surfaces, was used as a proxy for rhizosphere soil volume, named here rhizosphere soil matrix. It was then used in comparisons with the rhizosheath soil mass.

2.4 Statistics

The effects of plant species (*P. virgatum* vs. *R. hirta*), soil structure (sieved vs. intact), soil origin (switchgrass soil vs. prairie soil) and the type of process leading to changes in local macroporosity (root-induced changes vs. root growth preferences) on 1) macroporosity changes at distances of 0.0-0.1 mm and 2) 0.1-0.3 mm from the root were investigated using a linear mixed model approach implemented in the lme4 package (Bates *et al.*, 2015) of R (V. 4.1.1). Random effects included the planted pots, used as an error term for testing the plant species effect, and the ingrowth cores nested within the pots, used as an error term for testing the effects of soil structure and origin. In the same way, but without the factor of the type of process differences in rhizosheath dry weights were tested. The assumptions of normality and homogeneity of variances were assessed using normal probability plots of the residuals and Levene’s tests for equal variances. The rhizosheath weight was log-transformed, as the normality assumption was found to be violated. When the equal variance assumption was violated, the unequal variance models were fitted using nlme package in R (Pinheiro & Bates, 2000; Pinheiro *et al.*, 2024). When interactions between the studied factors were statistically significant ($P < 0.05$), simple effect F-tests

were conducted, followed by t-tests for multiple comparisons among the mean values using the emmeans package (Lenth, 2024). To explore the associations between local root-induced changes and the overall macroporosity, linear regression models were fitted separately for each distance increment.

To analyze for properties associated with rhizosheath dry weights, linear regressions of the rhizosheath dry weight were computed with the shares of roots grown into soil regions with different pore structures (i.e., soil matrix, macropores, biopores), with the root-induced changes as well as root growth preference effect separately for each distance increment. In addition, we conducted linear regression analysis of the associations between the rhizosheath dry weight and the X-ray µCT-derived soil volume (matrix soil without macroporosity) in 0.0-0.3 mm distance, which served as a proxy for the total rhizosphere soil matrix. The size of the rhizosphere, defined as the soil directly influenced by the root, largely depends on the process being investigated (Hinsinger *et al.*, 2009; Marschner, 2012; Kuzyakov & Razavi, 2019). Notably, previous studies have shown that macroporosity and carbon within the rhizosphere are particularly affected up to a distance of 0.3 mm (Koebernick *et al.*, 2019; van Veelen *et al.*, 2019; Moran *et al.*, 2022), in agreement with the analyzed gradients in macroporosity, which reached bulk macroporosity in most cases at distances >0.3 mm (Fig. 2).

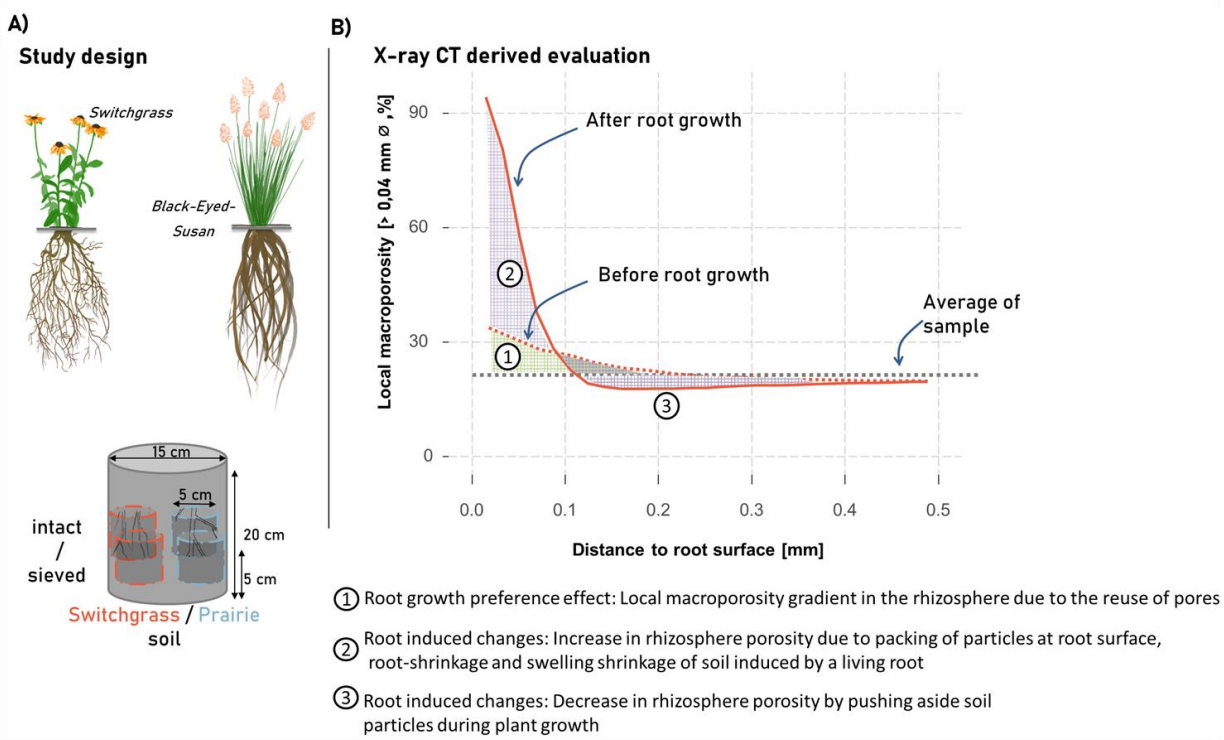

Figure 1: Outline of the study's experimental design (A) and of the methodological approach developed for quantification of root-induced changes and the root *growth preference effect* (B). (A) *R. hirta* and *P. virgatum* were planted into containers filled with 2-mm sieved soil and holding perforated ingrowth cores with soil of four contrasting pore structure characteristics, namely: intact and sieved soils of prairie and switchgrass origin. To ensure that the intact and sieved cores differed from each other only in terms of pore structure, the sieved soil was packed to the same bulk density as the intact cores and all >2 mm inclusions, such as stones and large root residues were incorporated back into the sieved soil prior to packing. B) Schematic representation of the approach used to evaluate macroporosity gradients around roots using X-ray µCT. The ingrowth cores were scanned twice to derive macroporosity profiles before and after root growth. The soil induced root *growth preferences effect* on these macroporosity gradients (1) is the difference between the average macroporosity of the core and the local macroporosity around the root. The changes induced by plants (2,3) are the difference between the macroporosity profiles before and after root growth.

Table 1: Summary of plant and root growth pattern characteristics (reported in Lucas *et al.*, 2023). Depicted are means and standard errors of shoot and root weights (n=6) for *R. hirta* and *P. virgatum* and their root length in the soils of the two studied origins (Switchgrass = SG and Prairie = PR soil) and structures (intact and sieved). In addition, the share of roots grown into soil matrix (< 0.04 mm Ø pores), macropores (> 0.04 mm Ø), and biopores is reported as % of the total root volume. Different letters mark significant differences between the studied plants for shoot and root weights as well as among the studied plant, origin, and structure combinations for the rest of the data (p<0.05).

Plant specie	Soil structure	Soil origin	Shoot weight (g)	Root weight (g)	Root length (mm)	Share of roots newly grown into		
						soil matrix (%)	macro-pores (%)	biopores (%)
R. hirta	intact	SG	2.66 ± 0.48	0.89 ±0.22**a**	2.77 ±0.1**bc**	59.22 ±1.21**bc**	22.34 ±0.94 **abc**	18.43 ±0.51**ab**

		PR			3.25 ±0.11**bc**	67.69 ±1.61**c**	14.69 ±0.63**a**	17.63 ±1.4**ab**
	sieved	SG			1.93 ±0.09**b**	62.84 ±1.08**c**	37.16 ±1.08**bcd**	NA*
		PR			2.65 ±0.17**c**	61.11 ±0.54**bc**	38.89 ±0.54**cd**	NA
	intact	SG			0.54 ±0.04**a**	36.45 ±1.43**a**	28.25 ±1.99**abc**	35.3 ±2.57**b**
		PR			0.59 ±0.04**a**	64.75 ±1.36**c**	18.46 ±0.99**ab**	16.79 ±1.56**a**
P. virgatum	sieved	SG	1.55 ±0.12	0.3 ±0.03**b**	0.34 ±0.06**a**	38.88 ±3.49**ab**	61.12 ±3.49**e**	NA
		PR			0.22 ±0.02**a**	48.26 ±2.43**abc**	51.74 ±2.43**e**	NA

*** Note, sieved soil cores did not contain any pre-existing biopores.**

3 Results

3.1 Rhizosphere gradients

Gradients in macroporosity at the locations later populated by roots were already observed prior to root growth, and across all investigated soil origins and structures the macroporosity near these locations was higher compared to the average macroporosity (Fig. 2). Root growth further modified these gradients, particularly within the 0.0-0.1 mm distance from the root surface, where a significant increase in macroporosity was observed for both plants across all four soil origins and structures.

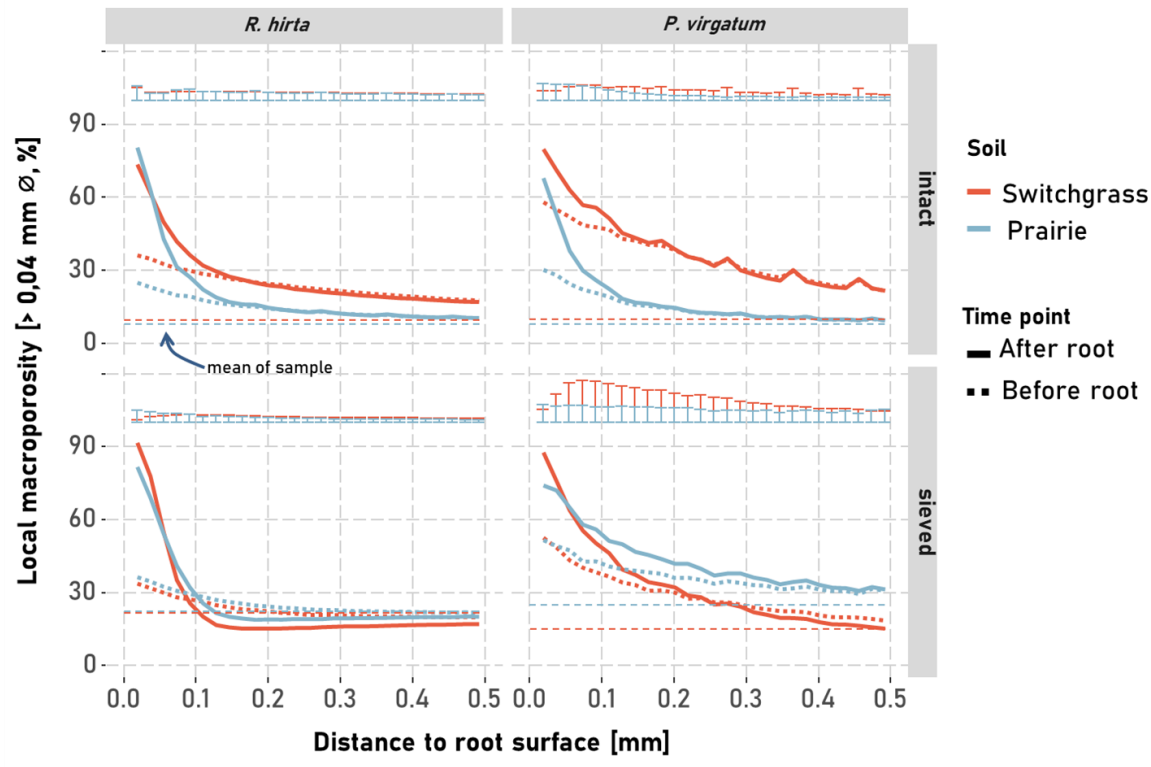

Figure 2: Gradients of the local macroporosity (pores >0.04 mm) with distance to the root surface of *Panicum virgatum* and *Rudbeckia hirta* when grown in sieved or intact soil of prairie or switchgrass origin. Gradients computed before (dotted line) and after root development are shown, along with average total macroporosity (dashed line). Error bars represent the standard errors of the local macroporosity means after root growth (n=6).

From the curves in Fig. 2, we calculated the extent of both effects: root growth preference and root-induced changes in the rhizosphere at 0.0-0.1 mm and 0.1-0.3 mm distances from the root. As expected, the local macroporosity changes from the root growth preference effect was strongly negatively correlated with the proportion of roots grown into the soil matrix, i.e., the soil areas lacking macropores, at both 0.0-0.1 mm (R^2=0.71, $p < 0.001$, Fig. S2A) and 0.1-0.3 mm (R^2=0.4, $p < 0.001$, Fig. S2B) distances. In contrast, root-induced changes on local macroporosity were positively associated with the proportion of roots grown into the soil matrix at 0.0-0.1 mm (R^2=0.4, $p < 0.001$, Fig. S2C), but not at 0.1-0.3 mm distance ($R^2 < 0.01$, $p = 0.56$).

At 0.0-0.1 mm, both root-induced changes and the root growth preferences effect resulted in higher macroporosity, ranging between 10% and 40% (Fig. 3A). Interestingly, root-induced changes within the 0.0-0.1 mm distance were similar for *R. hirta* and *P. virgatum*,

regardless of the soil structure or origin, resulting in an increase in the local macroporosity between 20% and 30%. In comparison, variations of the root growth preference effect within the 0.0-0.1 mm distance to the root were high (Fig. 3A). For instance, root growth preferences of *R. hirta* resulted in higher observed rhizosphere macroporosity by ~10% in sieved soil, while *P. virgatum* increased local macroporosity by over 40% in switchgrass soil, more than double the effect in prairie soil. Consequently, *R. hirta* root-induced changes at 0.0-0.1 mm were always higher or as high as the root growth preference effect, while the root growth preference effect of *P. virgatum* indirectly affected local macroporosity to a much greater extent compared to direct root-induced changes when grown in intact switchgrass soil.

At 0.1-0.3 mm from the root, the changes in macroporosity were strongly plant-dependent (Table S1), and the two processes showed distinct, sometimes opposing, patterns (Fig. 3B). Root growth preferences consistently resulted in higher rhizosphere macroporosity across all treatments. However, root-induced changes had minimal effects at 0.1-0.3 mm in structured soils for both species but diverged in sieved soils. Here, *R. hirta* reduced macroporosity, while *P. virgatum* further increased macroporosity (Fig. 3B). The negative effect of *R. hirta* on macroporosity in sieved soil was greater than the positive impact of the root growth preference effect, resulting in the observed overall local compaction at distances of > 0.1 mm in this treatment (Fig. 2).

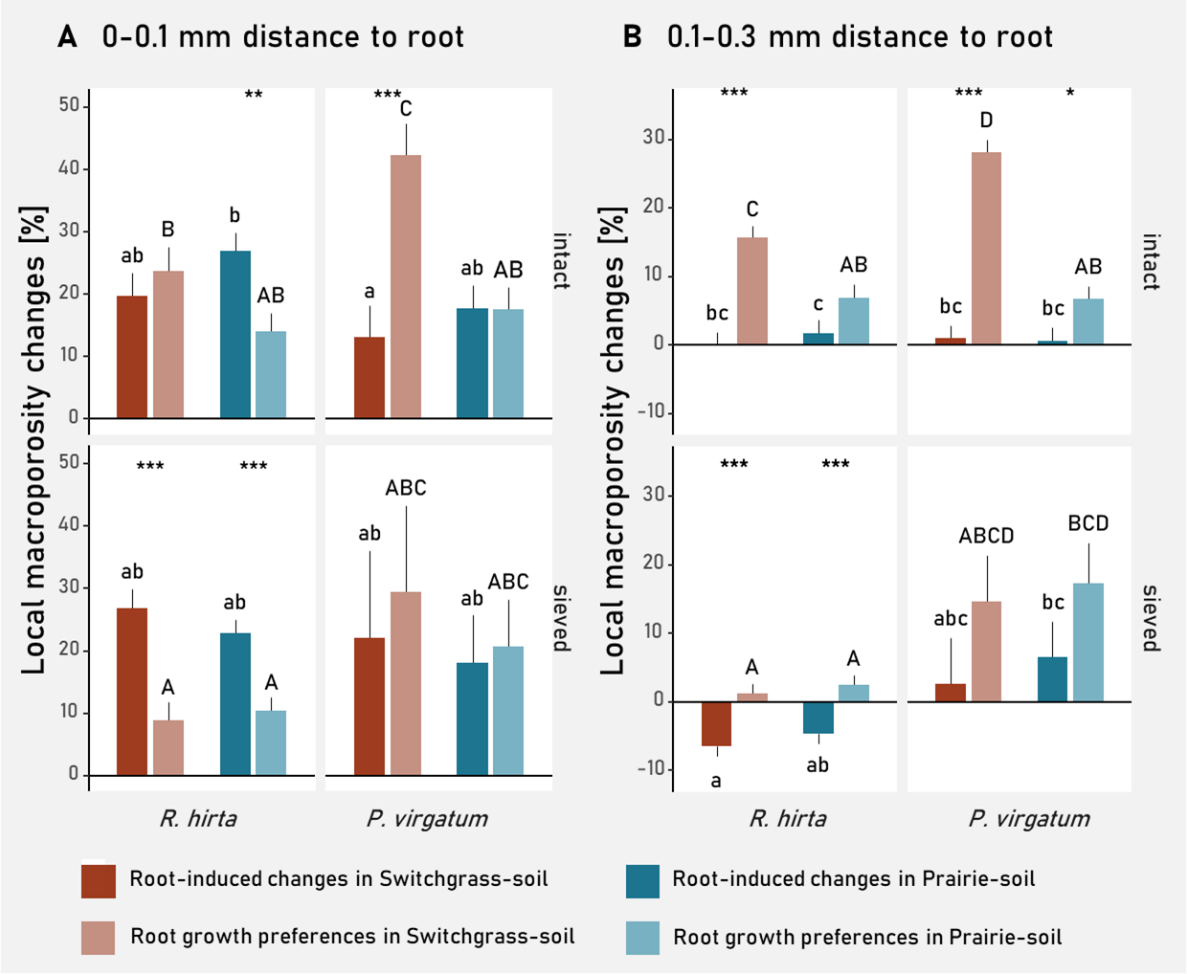

Figure 3: Local macroporosity changes (pores >0.04 mm diameter) due to the root growth preference effect and root-induced changes at 0.0-0.1 mm (A) and 0.1-0.3 mm (B) distances from the root surface of *P. virgatum* and *R. hirta* when grown in sieved or intact soil of prairie or switchgrass origin. Local macroporosity changes are calculated as described in Fig. 1. Different letters mark significant differences among plant species, soil structure, and soil origin combinations within each distance (P < 0.05). Capital letters correspond to the root growth preference effect and lowercase letters to root-induced changes. Asterisk indicate significant differences between the root-induced changes and the changes resulting from root growth preferences. Whiskers represent the standard errors of the mean (n=6).

3.2 Effects on Narrow pores (0.04-0.15 mm)

The volume of the narrow pores (0.04-0.15 mm diameter) was generally low, especially in intact soil structures (Fig. S3), thus the root growth preference effect was rather minor (<5%, Fig. 4) for both *P. virgatum* and *R. hirta*. In sieved soil, however, *P. virgatum*'s root growth preferences negatively impacted these pores, whereas *R. hirta* root growth preferences resulted in higher volumes of narrow pores (Fig 4A,B). Interestingly, during

plant growth, root-induced changes led to similar patterns for the narrow pores (Fig. S3) as compared to all macropores (Fig. 2), with a stark increase in these pore sizes close to the root surface and hardly any changes in intact soil in comparison to a compaction in the sieved versions of the soils in 0.1-0.3 mm distance (Fig. 4B).

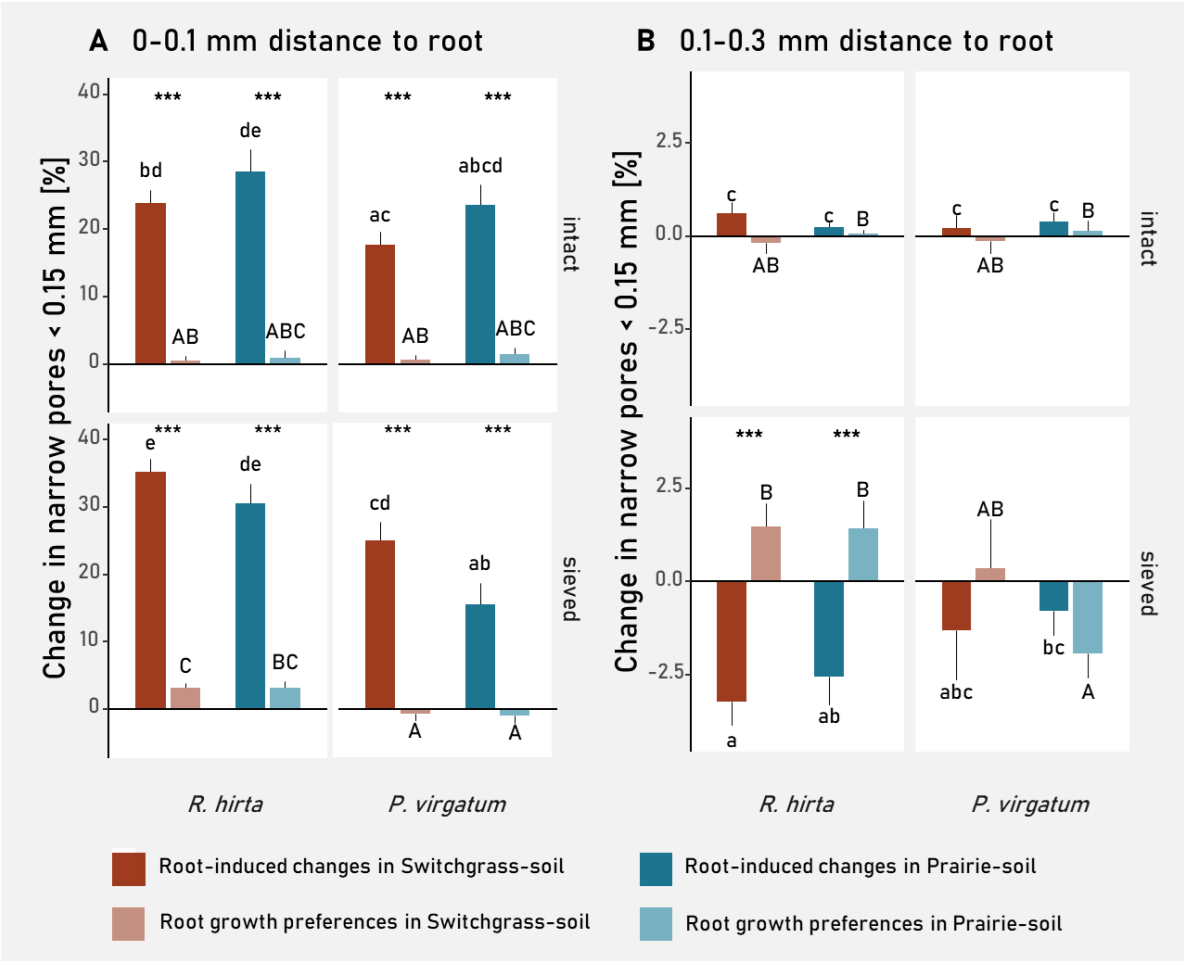

Figure 4: Local changes in narrow pores (0.04-0.15 mm diameter) due to the root growth preference effect and root-induced changes at 0.0-0.1 mm (A) and 0.1-0.3 mm (B) distances from the root surface of *P. virgatum* and *R. hirta* when grown in sieved or intact soil of prairie or switchgrass origin. Local porosity changes are calculated as described in Fig. 1. Different letters mark significant differences among plant species, soil structure, and soil origin combinations within each distance (P < 0.05). Capital letters correspond to root growth preference effect and lowercase letters to root-induced changes. Asterisk indicates significant differences between the root-induced changes and the changes resulting from the root growth preference effect. Whiskers represent the standard errors of the mean (n=6).

3.3 Impact of Root-Induced Changes on macroporosity

There were no significant differences in total macroporosity between the two plant species and the unplanted controls in any of the investigated soil structures (Fig. 5A). However,

while macroporosity in intact soil cores remained unchanged (Switchgrass soil) or numerically increased (Prairie soil), all sieved soil cores exhibited a reduction in macroporosity during plant root growth. Interestingly, only root-induced changes at 0.1-0.3 mm distance were positively associated with changes in the total macroporosity (Fig. 5B), whereas changes in macropores at 0.0-0.1 mm distance did not show this association (Fig. S4).

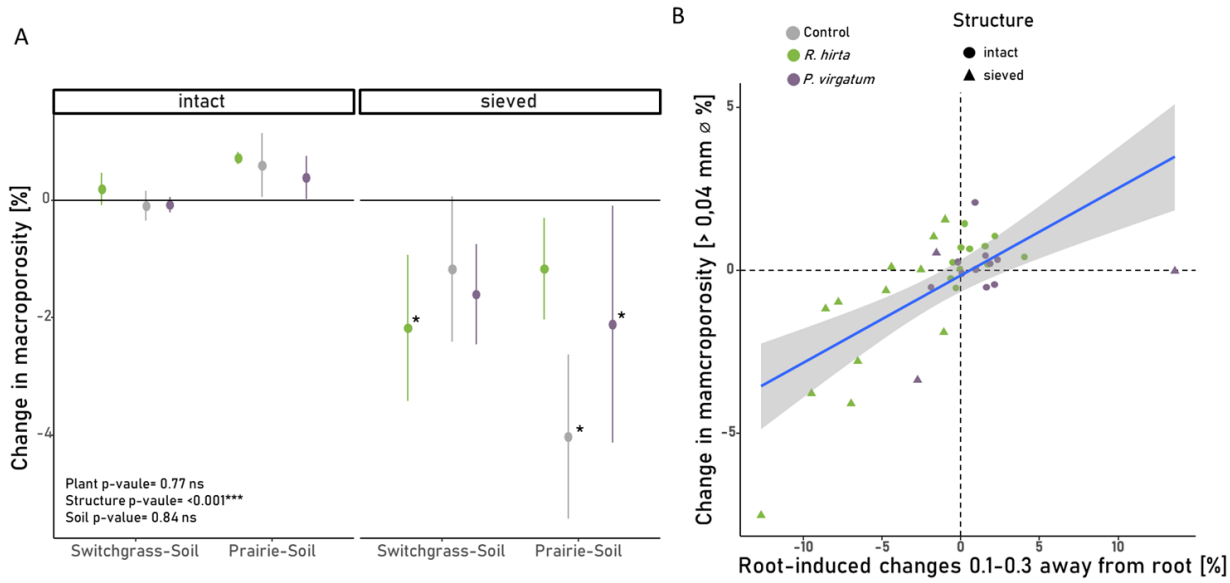

Figure 5: A) Changes in total macroporosity in cores from *P. virgatum*, *R. hirta*, and the unplanted control for the sieved and intact soils of prairie or switchgrass origin. There were no significant differences between plant species and soil origin combinations within each structure, but the effect of structure was significant, as indicated in the lower left part of the plot (P < 0.001). Stars indicate significant differences to zero. b) Association of root-induced changes of local macroporosity at 0.1-0.3 mm distance from the root with the change in total macroporosity after plant growth. Samples with root length <10 cm per core were excluded as their influence on total macroporosity was considered negligible.

3.4 Rhizosheath formation and it's relation to rhizosphere properties

Rhizosheath dry weight exhibited high variability, with significantly lower values for *R. hirta* grown in intact Prairie soil and sieved Switchgrass soil compared to *P. virgatum* grown in sieved Switchgrass soil (Fig. 6A). Surprisingly, there was no correlation between the µCT-derived rhizosphere soil matrix (matrix voxels within 0.0-0.3 mm away from the root) and rhizosheath dry weight (Fig. 6B). When considering only the distance up to 0.1 mm, rhizosheath dry weight for *R. hirta* was negatively correlated with the µCT-derived rhizosphere soil matrix (Fig. S5a).

However, for both plants the rhizosheath weight was positively correlated with plant-derived C, i.e. ^{14}C activity, in it (Fig. 6C), and with the proportion roots growing into macropores (Fig. 6D). There were no significant associations between the proportion of roots in biopores or the soil matrix and the rhizosheath dry weight. Similarly, we found no association of the root growth preference effect on the rhizosheath dry weight (Fig. S7 C and D). However, while an increase in macroporosity by root induced changes of *P. virgatum* negatively influenced rhizosheath dry weight in 0.0-0.1 mm distance to the root (Fig. S7A), there was no association for *R. hirta*. In contrast, at 0.1-0.3 mm distance, *R. hirta* positive changes on macroporosity were associated with a reduction in rhizosheath weight, while there was no association within the rhizosphere of *P. virgatum* (Fig. S7B).

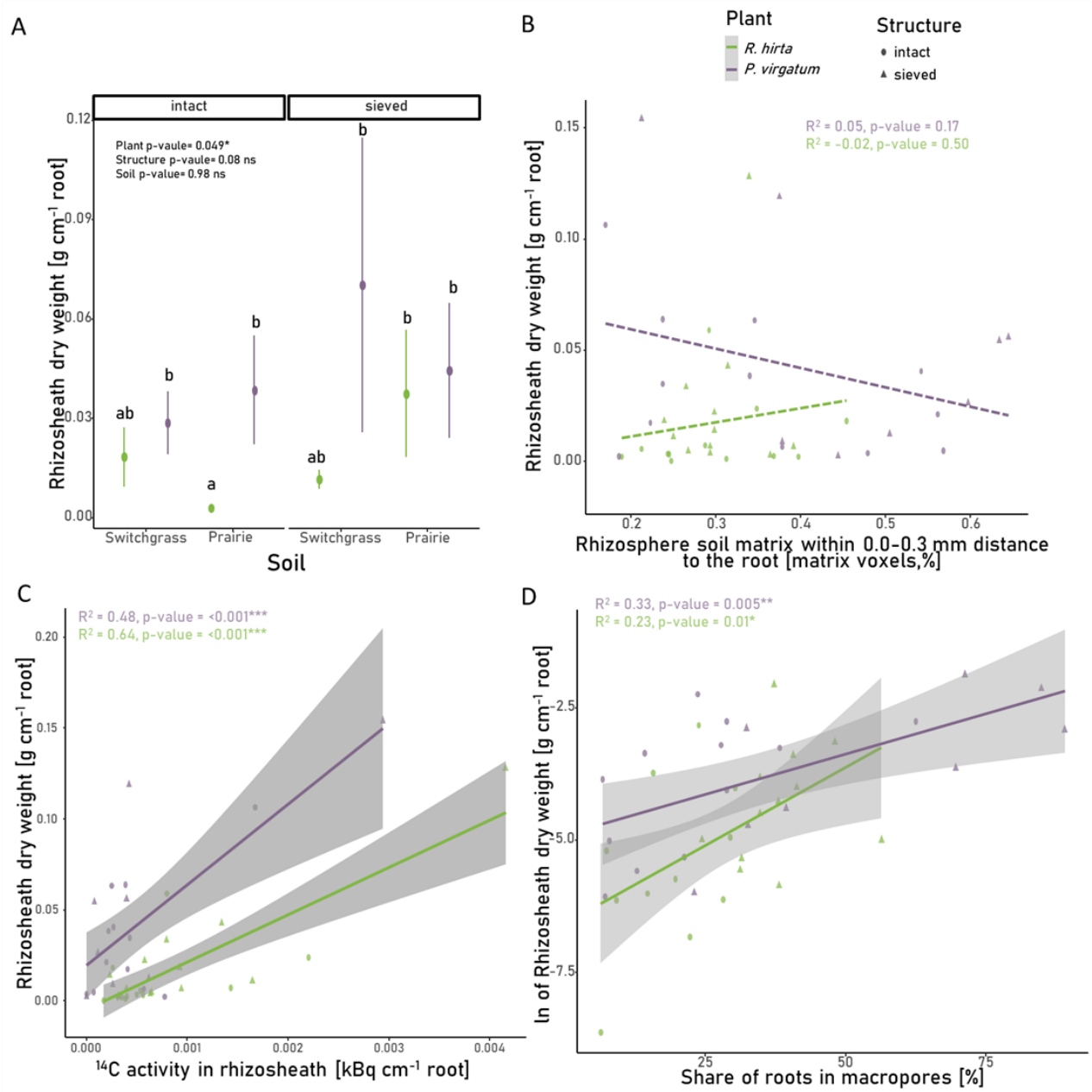

Figure 6: Rhizosheath development of P. virgatum and R. hirta. a) Rhizosheath weight of P. virgatum and R.hirta roots grown into intact and sieved soil of the two studied origins. Shown are mean values and standard errors. The letters indicate significant differences among the plant, structure, and soil origin combinations (P-value < 0.05). b) Rhizosheath dry weights plotted vs. the rhizosphere soil matrix, where the latter are estimated as the volumes of soil within 0.0-0.3 mm distance to root surfaces. c) Plant-derived C, represented by ^{14}C activity, in the rhizosheath plotted vs. the rhizosheath weight. d) Share of roots grown into macropores plotted vs. the rhizosheath weights. In b)-d) dots are the observed data and lines are the linear regression models fitted to them. Solid and dash lines represent, respectively, the linear regressions statistically significant or not at P-value<0.05.

4 Discussion

4.1 Root-induced vs. root growth preference-driven porosity gradients in the rhizosphere

Our findings from the sieved soil align well with previous studies exploring rhizosphere characteristics in similarly finely sieved and repacked soil settings (Helliwell *et al.*, 2017; Koebernick *et al.*, 2017, 2019; Phalempin *et al.*, 2021). However, by using repeated X-ray µCT imaging, we were able to describe rhizosphere macroporosity gradients forming upon new root growth, especially in natural, intact field soil. The approach made this study the first to distinguish between root-induced changes in rhizosphere macroporosity and the macroporosity gradients resulting from the root growth preference effect.

The results partially supported our first hypothesis demonstrating that root-induced changes indeed made an overall smaller contribution to formation of the rhizosphere porosity gradients as compared to that from root growth preferences. However, the relative contributions of the two mechanisms depended on the position within the rhizosphere, i.e., at 0-0.1 mm vs. 0.1-0.3 mm distances from the root surfaces. At/close to the root-interface, i.e., at 0.0-0.1 mm distance, direct influences of roots on the rhizosphere macroporosity were comparable or even bigger (in sieved soil) as the root growth preference effect (Fig. 3A). These local root-induced changes may be a combined result of enhanced shrinkage and swelling of the soil, rhizodeposition, root hair growth and root shrinkage (Carminati *et al.*, 2013; Koebernick *et al.*, 2017; Helliwell *et al.*, 2019). However, when a larger proportion of roots elongated into the soil matrix and the root growth preference effect on macropores within 0.0–0.1 mm from the root surface was minimal (Fig. S2A), root-induced changes were highest (Fig. S2C). These changes appeared to be primarily driven by the formation of pores of a specific size, namely narrow pores (Fig. 4A). This suggests that geometric factors strongly influence the root-induced changes at the root-soil interface for roots growing into the soil matrix (Koebernick *et al.*, 2019). When roots push aside and rearrange soil upon their growth through the soil matrix, the rearrangement and packing structure of the relatively spherical soil particles along the flat root surface naturally lead to increased porosity at the immediate root interface—a phenomenon described as the surface-wall effect (Koebernick *et al.*, 2019; Lucas *et al.*, 2019). Conversely, when roots predominantly utilized existing macropores, root-induced

changes in 0.0-0.1 mm distance were minimal (Fig. S2A,C). This was especially evident in the case of *P. virgatum* growing into soil previously occupied by switchgrass (Fig. 3A, top). Here, the extensive reuse of existing macro- and biopores (Table 1) maximized the root growth preference effect while simultaneously minimizing root-induced changes.

Farther away from the root surface (0.1-0.3 mm distance) the root-induced impact on macroporosity substantially deviated in size and direction from the root growth preference effect (Fig. 3B). The strong negative correlation between the root growth preference effect and the proportion of roots growing in the soil matrix (Fig. S2B) further emphasized that the roots' preference to grow into more porous and macropore abundant areas was the primary driver of the observed local macroporosity gradients in the rhizosphere. This finding underscores the importance of the interactions between roots and the inherent pore structure of the intact soil in defining rhizosphere pore characteristics (Lucas *et al.*, 2019; Phalempin *et al.*, 2021). In other words, the amount and connectivity of macropores and their re-use by the root system are the main determinants of the physical properties of the rhizosphere.

Our comparison of intact and sieved soil structures further emphasized that the complex effects of roots on physical characteristics of the rhizosphere result from their interaction with the existing pore structure. In general, soil compression mainly reduces large structural macropores, with a lesser impact on meso- and micropores within the soil matrix (Kutilek *et al.*, 2006). However, macropores that are as large as, or larger than, the roots themselves can be reused by roots and are therefore typically not compacted during root growth (Lucas *et al.*, 2022). Thus, it is primarily the volume of narrow pores that is affected by root compaction. In the sieved soil, these narrow pores were the ones primarily compacted by plant roots (Fig. S4, Fig. 4B bottom part). In contrast, in intact field soils where many roots grew into existing biopores (Lucas et al. 2023) and where the narrow pores were less abundant, root-induced changes on macropores in the rhizosphere by roots were minimal (Fig. 4B top part, 5A). This explains why a compacted rhizosphere zone is typically observed in finely sieved soils with a large amount of narrow pores (Koebernick *et al.*, 2019; Lucas *et al.*, 2019) but is absent in loosely packed or coarsely structured soils with many large macropores, as well as in field soils with biopores (Lucas

et al., 2019; Phalempin *et al.*, 2021). The lack of a compaction zone in intact samples is, therefore, a result of fewer narrow pores and of more well-connected biopores available for reuse. While previous studies suggested that coarse root systems induce higher local compaction (Dexter, 1987; Lucas *et al.*, 2019), our results demonstrate that even for coarse rooted plants, such as *P.virgatum*, the reuse of existing pores, with resultant lack of root-induced compaction, can be the main factor shaping rhizosphere macroporosity.

The macroporosity gradients in the rhizosphere show a strikingly consistent pattern across different soil structures, particularly for narrow pores (Fig. S3). In both intact and sieved soils, the volume of such pores increases sharply close to the root surface tapering down to very low values at 0.1–0.2 mm. In intact soils, such low values results from the low amount of narrow pores in the bulk soil, while in sieved soils, it is primarily due to root-induced compaction (Fig. 4B bottom part). Although intact and sieved soils initially displayed different porosity patterns, they have now converged to a remarkably similar profile, likely due to the interplay between root growth preferences and root-induced changes that counterbalance each other's effects (Fig. S2A, C).This finding aligns with the concept of a self-organizing rhizosphere, which optimizes conditions for microbial habitats and water movement (Rabbi *et al.*, 2018b). Young & Crawford (2004) introduced the idea of a self-organizing soil-microbe complex as the interconnected relationship between soil's physical structure (e.g., its pore network) and microbial life. As microbes break down organic matter and interact with root carbon inputs, they can reorganize the soil's pore structure. This reorganization affects how water, nutrients, and air move through the soil, in turn affecting the plants and the microbes themselves. The two systems—biological and physical—are therefore intertwined, constantly influencing each other in the rhizosphere environment (Young & Crawford, 2004; Rabbi *et al.*, 2018b). Our results demonstrate that a joint impact of the root growth preference effect and root-induced changes modifies rhizosphere pore structure by increasing proportions of narrow (0.04-0.15 mm diam.) pores in close proximity to the roots, that is, exactly in the locations where root exudates and rhizodeposits are released. Thus, soil-root-microbe interface provides an optimal environment for microbial activity, making root surfaces and their immediate vicinity particularly active microbial hotspots (Schmidt *et al.*, 2018; Mueller *et*

al., 2024). The reduction of small pores in the 0.1-0.3 mm zone may reduce water flow towards the roots. However, model simulations by Landl et al. (2021) suggest that this reduction can lead to prolonged periods of lower transpiration, which could ultimately be beneficial for the plant by preventing rapid dehydration. In summary, the interactions between the root growth preference effect and root-induced changes play a key role in the self-organization of the rhizosphere, establishing favorable physical conditions for nutrient acquisition and water uptake by plants across both sieved and intact soil structures (Rabbi *et al.*, 2018b; van Veelen *et al.*, 2019; Landl *et al.*, 2021).

4.2 Changes in total macroporosity

Consistent with our first hypothesis, minimal changes in the total macropororsity were observed in intact soils, with no differences from unplanted controls (Fig. 5A). Past studies reported high variability in plant induced changes in macroporosity, depending on the plant type and soil pore structure (Bodner *et al.*, 2014; Lucas *et al.*, 2022). Yet, consistent with our results, when there is a well-developed macropore system, plants seem to reuse and rearrange the existing pore space rather than create new macropores (Lucas, 2020; Lucas *et al.*, 2022).

However, the total macroporosity in the sieved samples decreased upon root growth (Fig. 5A), and the reduction in the local macroporosity at greater (i.e., 0.1-0.3 mm) distances from the roots apparently reduced the total macroporosity (Fig. 5B). Even though, numerous pores were created immediately at the root surface (i.e., at 0-0.1 mm distance) (Fig. 3A), they did not increase the total macroporosity (Fig. S4). Thus, it can be surmised that they were created at the expense of other pores, compacting the rest of the rhizosphere soil.

4.3 Rhizosheath Development

Our second hypothesis was supported by the data, and we observed strong positive associations between the rhizosheath mass and the quantities of root-derived carbon in it (Fig. 6c) as well as tendencies for greater rhizosheath mass to cooccur with greater root-induced reduction in rhizosphere macroporosity (Figs. S7A, B). These results probably

reflect a joint outcome of soil particles being pushed aside by the growing roots and being glued together by plant-released organic compounds and root hairs (York *et al.*, 2022; Aslam *et al.*, 2022). Although root hairs were not measured here, previous studies suggest that they develop in patchy patterns, and can be particularly long in areas with low soil contact, such as macropores (Duddek *et al.*, 2024). Indeed, when a large proportion of roots grew into macropores, the rhizosheath mass was positively impacted (Fig. 6D), while the increase in plant-originated carbon found within the rhizosheath (Fig. 6C) might in part reflect the presence of detached root hairs. Another factor potentially explaining the association between roots grown in macropores and rhizosheath mass is that, in sieved soil, most macropores are narrow pores, which are smaller compared to many roots (Lucas *et al.*, 2023). Thus, as *R. hirta* roots grew into narrow-pore regions, they displaced soil particles, locally reducing macroporosity (Fig. S7B). This generated similar rhizosphere macroporosity profiles in both intact and sieved soils as elaborated above, but encouraged rhizosheath formation only in the sieved soil

Our third hypothesis, however, was not supported, as we found no relationship between rhizosheath mass and the µCT-derived rhizosphere soil volume (Fig. 6B). This lack of association might be a result of rhizosheath formation being only influenced by root-induced changes, not by the root growth preference effect. While variations in root growth into the soil matrix significantly impacted rhizosphere structure (Figs. S2A, B), they did not affect rhizosheath development (Figs. S6B and S7C, D). Rhizosheath soil is therefore not associated with the rhizosphere structure, as the latter is affected by both, directly through root-induced changes and indirectly through root growth preferences. Only the µCT-derived rhizosphere soil matrix within 0.0-0.1 mm (previously used as a proxy for soil contact, Lucas *et al.*, 2023) of the roots of *R. hirta* correlated with rhizosheath dry weight, and this correlation was negative (Fig. S5A). Similarly, Rabbi et al. (2018b) observed increased macroporosity near roots and higher rhizosheath mass in drought-tolerant species compared to drought-sensitive species, attributing these differences to mucilage acting as a glue between soil particles and stabilize particles during drying.

It is important to note that our imaging resolution did not capture pores smaller than 0.04 mm. Yet, as the macropore volume varied drastically (>50 vol%, Fig. 6b), the

corresponding rhizosheath mass should have had decreased with increasing macroporosity. Furthermore, our resolution did not permit visualization of root hairs or their contribution to root-soil contact. However, given our voxel size (0.0182 mm), the majority of pores in the soil matrix would be water-filled, making the soil within 0.0–0.1 mm a reasonable proxy for root-soil contact (Lucas *et al.*, 2023).

In summary, and contrary to the common assumption our data does not support the notion that rhizosheath mass is a proxy for rhizosphere structure or soil contact in general. Rather, rhizosheath formation seems to occur primarily around roots that actively reshape their surroundings and enhance soil contact by reducing macroporosity. In contrast, roots growing into the soil matrix do not need to modify the already dense rhizosphere, and this soil does not tend to remain attached during rhizosheath sampling. Thus, while rhizosheath mass may indicate improved soil contact in high-macroporosity soils, such as sands (Price, 1911; Buckley, 1982) it is not an representative for the rhizosphere of an entire root system in finer-structured soils.

4.4 Implications for further rhizosphere and rhizosheath focused research

Our study provides new insights into complex interactions between root growth patterns, rhizosphere macroporosity, and rhizosheath formation. We demonstrated that root interactions with inherent pore structure play a crucial role in shaping rhizosphere properties, with root growth patterns, rather than direct root-induced changes, being the dominant factor influencing local macroporosity gradients. The distinction between root-induced changes and the root growth preference effect underscores the importance of considering not only how roots affect pore structure but also how pore structure influences root behavior. Given that in this study the effects of root growth preferences and root-induced changes varied significantly depending on whether the plant was growing in sieved or intact soil, we strongly advocate for the use of intact soil samples in rhizosphere research. Additionally, modeling approaches that explicitly incorporate rhizosphere soil structure will be essential for assessing the impact of root-soil interactions on water and nutrient dynamics at the plant scale.

Root architecture, hair development, and rhizodeposition are well known for their impact on rhizosphere characteristics; and recently these traits have been identified as key targets for breeding programs aimed at improving plant resilience (Lynch, 2019; York et al., 2016). Yet, as demonstrated by our study, root growth preferences within heterogeneous pore structure of intact soil can play an outsized role in plant-soil interactions, with potential impacts on plants' water and nutrient acquisition as well as on soil carbon inputs and cycling. These effects are currently overlooked by both plant breeding and soil health research efforts.

Due to challenges in rhizosphere sampling and quantification, researchers often use rhizosheath soil as a rhizosphere proxy (Hallett *et al.*, 2022; Mueller *et al.*, 2024). This approach assumes that root-adhering soil is representative of the entire rhizosphere (Pang *et al.*, 2017). However, our data suggest that this assumption might not be warranted. It appears that the rhizosheath formation predominantly occurs around roots growing into macropores of non-biological origin (Fig. 6D) and is potentially accompanied by development of dense root hairs to increase contact with the soil. On the other hand, the roots exploring biopores or growing into dense soil matrix are less likely to have soil firmly attached to them as the rhizosheath. Therefore, results obtained from analyses of rhizosheath material may not represent the entire rhizosphere, particularly not the roots with highly active laterals that have large root-soil contact in denser soil matrices. Future research should integrate structural analyses of the rhizosphere with rhizosheath studies to better understand the mechanisms driving root-soil interactions.

5 Data availability

All raw image data that support this study are available under doi: 10. 48758/ufz.13657.

6 Acknowledgements

This research was funded in part by the Great Lakes Bioenergy Research Center, U.S. Department of Energy, Office of Science, Office of Biological and Environmental Research under Award Number DE-SC0018409, by the NSF DEB Program (Award # 1904267), by the NSF LTER Program (DEB 1027253) at the Kellogg Biological Station, and by Michigan State University AgBioResearch.

We thank Maxwell Oerther for his great support during the whole experiment, Jinho Lee for his help on the field site and Michelle Quigley for her support during the X-ray µCT scans. We highly appreciate the help from the laboratories of Eric Patterson and Thomas Sharkey during the 14C analysis and 14C labelling, respectively.

7 Competing interests

The authors declare no competing interests.

8 Author contributions

A.G. and M.L. constructed and built the plant pots, ingrowth cores and cores for collecting soil water. M.L., A.K. and A.G. designed the experimental setup. M.L conducted the experimental work. All authors discussed the results and finalized the paper. A.K. and M.L. analyzed the data and wrote the paper.

9 References

Aravena JE, Berli M, Ghezzehei TA, Tyler SW. **2011**. Effects of root-induced compaction on rhizosphere hydraulic properties--X-ray microtomography imaging and numerical simulations. *Environmental science & technology* **45**: 425–31.

Aslam MM, Karanja JK, Dodd IC, Waseem M, Weifeng X. **2022**. Rhizosheath: An adaptive root trait to improve plant tolerance to phosphorus and water deficits? *Plant, Cell & Environment* **45**: 2861–2874.

Bodner G, Leitner D, Kaul H-P. **2014**. Coarse and fine root plants affect pore size distributions differently. *Plant and soil* **380**: 133–151.

Bruand A, Cousin I, Niccoullaud B, Duval O, Begon JC. **1996**. Backscattered Electron Scanning Images of Soil Porosity for Analyzing Soil Compaction around Roots. *Soil Science Society of America Journal* **60**: 895–901.

Buckley R. **1982**. Sand rhizosheath of an arid zone grass. *Plant and Soil* **66**: 417–421.

Carminati A, Vetterlein D, Koebernick N, Blaser S, Weller U, Vogel H-J. **2013**. Do roots mind the gap? *Plant and Soil* **367**: 651–661.

Cheraghi M, Mousavi SM, Zarebanadkouki M. **2023**. Functions of rhizosheath on facilitating the uptake of water and nutrients under drought stress: A review. *Plant and Soil*.

Dexter AR. **1987**. Compression of soil around roots. *Plant and Soil* **97**: 401–406.

Duddek P, Papritz A, Ahmed MA, Lovric G, Carminati A. **2024**. Observations of root hair patterning in soils: Insights from synchrotron-based X-ray computed microtomography. *Plant and Soil*.

Feeney DS, Crawford JW, Daniell T, Hallett PD, Nunan N, Ritz K, Rivers M, Young IM. **2006**. Three-dimensional microorganization of the soil-root-microbe system. *Microbial ecology* **52**: 151–8.

Hallett PD, Marin M, Bending GD, George TS, Collins CD, Otten W. **2022**. Building soil sustainability from root–soil interface traits. *Trends in Plant Science* **27**: 688–698.

Helliwell JR, Sturrock CJ, Mairhofer S, Craigon J, Ashton RW, Miller AJ, Whalley WR, Mooney SJ. **2017**. The emergent rhizosphere: imaging the development of the porous architecture at the root-soil interface. *Scientific reports* **7**: 14875.

Helliwell JR, Sturrock CJ, Miller AJ, Whalley WR, Mooney SJ. **2019**. The role of plant species and soil condition in the structural development of the rhizosphere. *Plant, cell & environment* **42**: 1974–1986.

Hildebrand T, Rüegsegger P. **1997**. A new method for the model-independent assessment of thickness in three-dimensional images. *Journal of Microscopy* **185**: 67–75.

Hinsinger P, Bengough AG, Vetterlein D, Young IM. **2009**. Rhizosphere: biophysics, biogeochemistry and ecological relevance. *Plant and Soil* **321**: 117–152.

Koebernick N, Daly KR, Keyes SD, Bengough AG, Brown LK, Cooper LJ, George TS, Hallett PD, Naveed M, Raffan A, *et al.* 2019. Imaging microstructure of the barley rhizosphere: particle packing and root hair influences. *The New phytologist* **221**: 1878–1889.

Koebernick N, Daly KR, Keyes SD, George TS, Brown LK, Raffan A, Cooper LJ, Naveed M, Bengough AG, Sinclair I, *et al.* 2017. High-resolution synchrotron imaging shows that root hairs influence rhizosphere soil structure formation. *The New phytologist* **216**: 124–135.

Koebernick N, Schlüter S, Blaser SRGA, Vetterlein D. **2018**. Root-soil contact dynamics of Vicia faba in sand. *Plant and Soil* **431**: 417–431.

Kravchenko AN, Guber AK, Razavi BS, Koestel J, Quigley MY, Robertson GP, Kuzyakov Y. **2019**. Microbial spatial footprint as a driver of soil carbon stabilization. *Nature communications* **10**: 3121.

Kutilek M, Jendele L, Panayiotopoulos K. **2006**. The influence of uniaxial compression upon pore size distribution in bi-modal soils. *Soil and Tillage Research* **86**: 27–37.

Kuzyakov Y, Razavi BS. **2019**. Rhizosphere size and shape: Temporal dynamics and spatial stationarity. *Soil Biology and Biochemistry* **135**: 343–360.

Landl M, Phalempin M, Schlüter S, Vetterlein D, Vanderborght J, Kroener E, Schnepf A. **2021**. Modeling the Impact of Rhizosphere Bulk Density and Mucilage Gradients on Root Water Uptake. *Frontiers in Agronomy* **3**.

Lenth RV. **2024**. *emmeans: Estimated Marginal Means, aka Least-Squares Means*.

Li Z, Kravchenko AN, Cupples A, Guber AK, Kuzyakov Y, Philip Robertson G, Blagodatskaya E. **2024**. Composition and metabolism of microbial communities in soil pores. *Nature Communications* **15**: 3578.

Lucas M. **2020**. *Soil structure formation through the action of plants*. Universitäts- und Landesbibliothek Sachsen-Anhalt.

Lucas M, Nguyen LTT, Guber A, Kravchenko AN. **2022**. Cover crop influence on pore size distribution and biopore dynamics: Enumerating root and soil faunal effects. *Frontiers in plant science* **13**: 928569.

Lucas M, Santiago JP, Chen J, Guber A, Kravchenko A. **2023**. The soil pore structure encountered by roots affects plant-derived carbon inputs and fate. *New Phytologist* **240**: 515–528.

Lucas M, Schlüter S, Vogel H-J, Vetterlein D. **2019**. Roots compact the surrounding soil depending on the structures they encounter. *Scientific reports* **9**: 16236.

Marschner P. **2012**. Rhizosphere Biology. In: Marschner's Mineral Nutrition of Higher Plants. Elsevier, 369–388.

Mo X, Wang M, Zeng H, Wang J. **2023**. Rhizosheath: Distinct features and environmental functions. *Geoderma* **435**: 116500.

Moran JJ, Linley TJ, Makarem CN, Kelly JF, Wilcox Freeburg ED, Cleary DM, Alexander ML, Kriesel JM. **2022**. Spectroscopy-based isotopic (δ13C) analysis for high spatial resolution of carbon exchange in the rhizosphere. *Rhizosphere* **23**: 100564.

Mueller CW, Baumert V, Carminati A, Germon A, Holz M, Kögel-Knabner I, Peth S, Schlüter S, Uteau D, Vetterlein D, *et al.* 2024. From rhizosphere to detritusphere – Soil structure formation driven by plant roots and the interactions with soil biota. *Soil Biology and Biochemistry*: 109396.

Ndour PMS, Heulin T, Achouak W, Laplaze L, Cournac L. **2020**. The rhizosheath: from desert plants adaptation to crop breeding. *Plant and Soil* **456**: 1–13.

Pang J, Ryan MH, Siddique KHM, Simpson RJ. **2017**. Unwrapping the rhizosheath. *Plant and Soil* **418**: 129–139.

Pankievicz VCS, Delaux P-M, Infante V, Hirsch HH, Rajasekar S, Zamora P, Jayaraman D, Calderon CI, Bennett A, Ané J-M. **2022**. Nitrogen fixation and mucilage production on maize aerial roots is controlled by aerial root development and border cell functions. *Frontiers in Plant Science* **13**: 977056.

Pausch J, Kuzyakov Y. **2011**. Photoassimilate allocation and dynamics of hotspots in roots visualized by 14 C phosphor imaging. *Journal of Plant Nutrition and Soil Science* **174**: 12–19.

Phalempin M, Lippold E, Vetterlein D, Schlüter S. **2021**. Soil texture and structure heterogeneity predominantly governs bulk density gradients around roots. *Vadose Zone Journal* **20**.

Pinheiro JC, Bates DM. **2000**. *Mixed-Effects Models in S and S-PLUS*. New York: Springer.

Pinheiro J, Bates D, R Core Team. **2024**. *nlme: Linear and Nonlinear Mixed Effects Models*.

Price SR. **1911**. THE ROOTS OF SOME NORTH APRICAN DESERT-GRASSES. *New Phytologist* **10**: 328–340.

Rabbi SMF, Tighe MK, Flavel RJ, Kaiser BN, Guppy CN, Zhang X, Young IM. **2018a**. Plant roots redesign the rhizosphere to alter the three-dimensional physical architecture and water dynamics. *The New phytologist* **219**: 542–550.

Rabbi SMF, Tighe MK, Knox O, Young IM. **2018b**. The impact of carbon addition on the organisation of rhizosheath of chickpea. *Scientific reports* **8**: 18028.

Ruamps LS, Nunan N, Pouteau V, Leloup J, Raynaud X, Roy V, Chenu C. **2013**. Regulation of soil organic C mineralisation at the pore scale. *FEMS Microbiology Ecology* **86**: 2635.

Santiago JP, Soltani A, Bresson MM, Preiser AL, Lowry DB, Sharkey TD. **2021**. Contrasting anther glucose-6-phosphate dehydrogenase activities between two bean varieties suggest an important role in reproductive heat tolerance. *Plant, cell & environment* **44**: 2185–2199.

Schmidt H, Nunan N, Höck A, Eickhorst T, Kaiser C, Woebken D, Raynaud X. **2018**. Recognizing Patterns: Spatial Analysis of Observed Microbial Colonization on Root Surfaces. *Frontiers in Environmental Science* **6**: 61.

Schnepf A, Carminati A, Ahmed MA, Ani M, Benard P, Bentz J, Bonkowski M, Knott M, Diehl D, Duddek P, *et al.* 2022. Linking rhizosphere processes across scales: Opinion. *Plant and Soil* **478**: 5–42.

van Veelen A, Koebernick N, Scotson CS, McKay-Fletcher D, Huthwelker T, Borca CN, Mosselmans JFW, Roose T. **2019**. Root-induced soil deformation influences Fe, S and P: rhizosphere chemistry investigated using synchrotron XRF and XANES. *New Phytologist*.

Vogel H-J, Weller U, Schlüter S. **2024**. Linking structure and functions in agricultural soils. In: Advances in Agronomy. Elsevier, 363–403.

Vollsnes AV, Futsaether CM, Bengough AG. **2010**. Quantifying rhizosphere particle movement around mutant maize roots using time-lapse imaging and particle image velocimetry. *European Journal of Soil Science* **61**: 926–939.

Watt M, McCully ME, Canny MJ. **1994**. Formation and Stabilization of Rhizosheaths of Zea mays L.'. **106**.

White RG, Kirkegaard JA. **2010**. The distribution and abundance of wheat roots in a dense, structured subsoil--implications for water uptake. *Plant, cell & environment* **33**: 133–48.

York LM, Cumming JR, Trusiak A, Bonito G, Von Haden AC, Kalluri UC, Tiemann LK, Andeer PF, Blanc-Betes E, Diab JH, *et al.* 2022. Bioenergy Underground: Challenges and opportunities for phenotyping roots and the microbiome for sustainable bioenergy crop production. *The Plant Phenome Journal* **5**: e20028.

Young IM, Crawford JW. **2004**. Interactions and Self-Organization in the Soil-Microbe Complex. *Science* **304**: 1634–1637.

Zhang Y, Du H, Gui Y, Xu F, Liu J, Zhang J, Xu W. **2020**. Moderate water stress in rice induces rhizosheath formation associated with abscisic acid and auxin responses. *Journal of experimental botany*.

A)

Study design

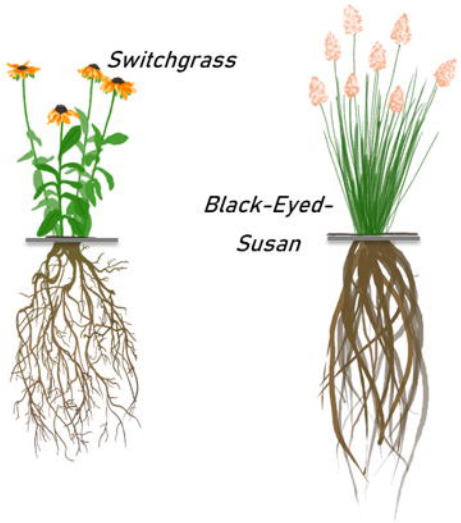

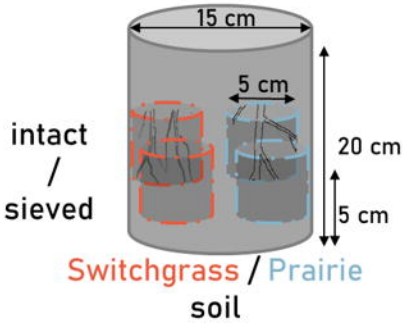

B)

X-ray CT derived evaluation

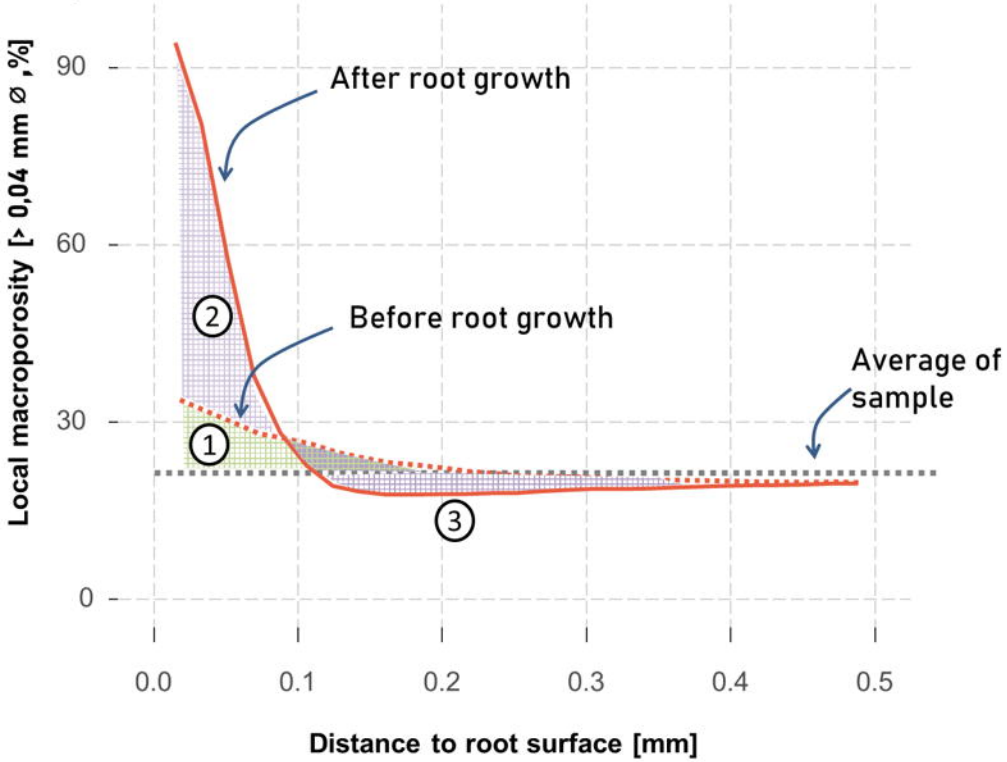

① Root growth preference effect: Local macroporosity gradient in the rhizosphere due to the reuse of pores

② Root induced changes: Increase in rhizosphere porosity due to packing of particles at root surface, root-shrinkage and swelling shrinkage of soil induced by a living root

③ Root induced changes: Decrease in rhizosphere porosity by pushing aside soil particles during plant growth

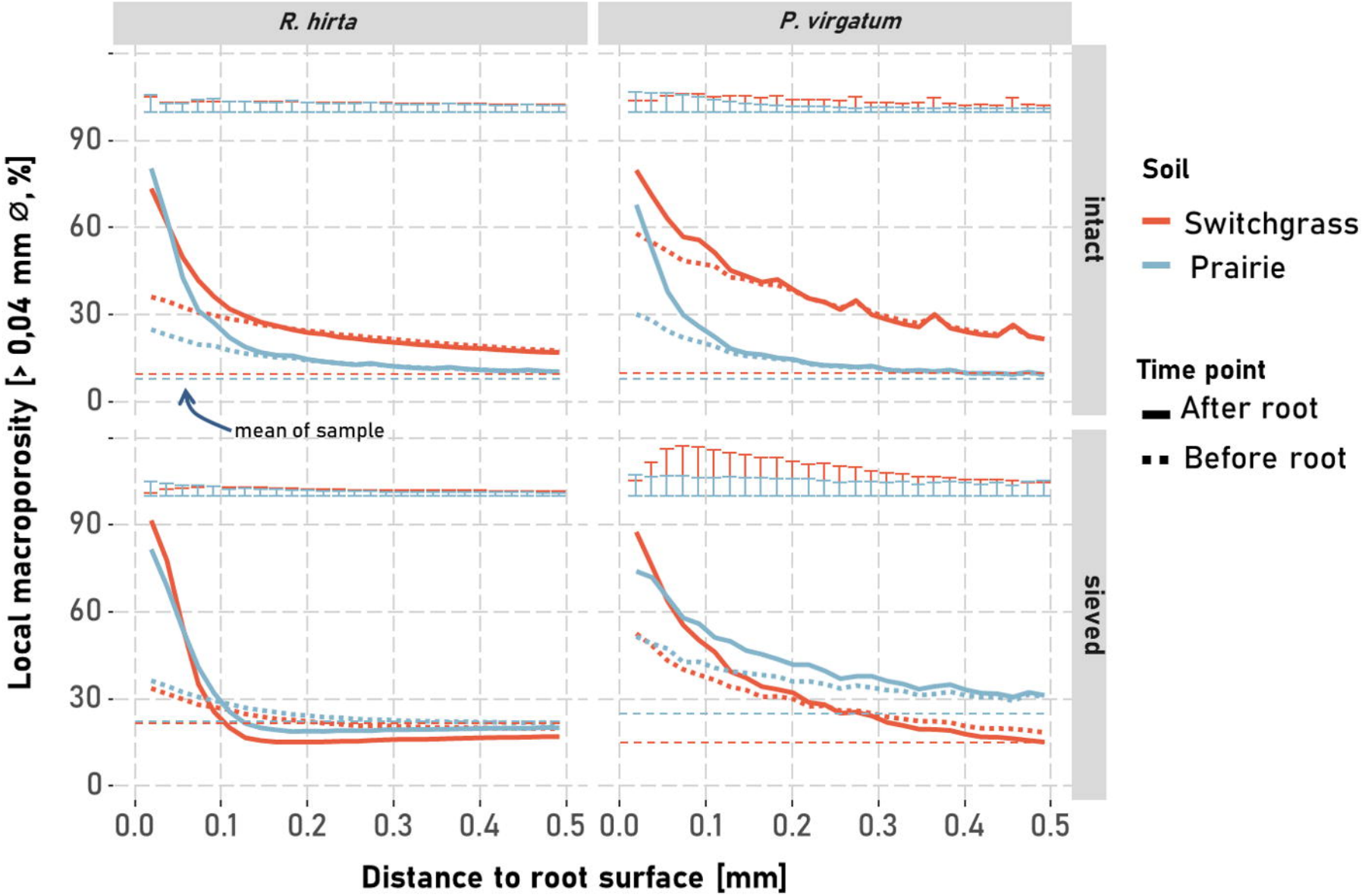
R. hirta
P. virgatum
intact
sieved
Local macroporosity [> 0,04 mm Ø, %]
90
60
30
0
mean of sample
0.0
0.1
0.2
0.3
0.4
0.5
Distance to root surface [mm]
Soil
Switchgrass
Prairie
Time point
After root
Before root

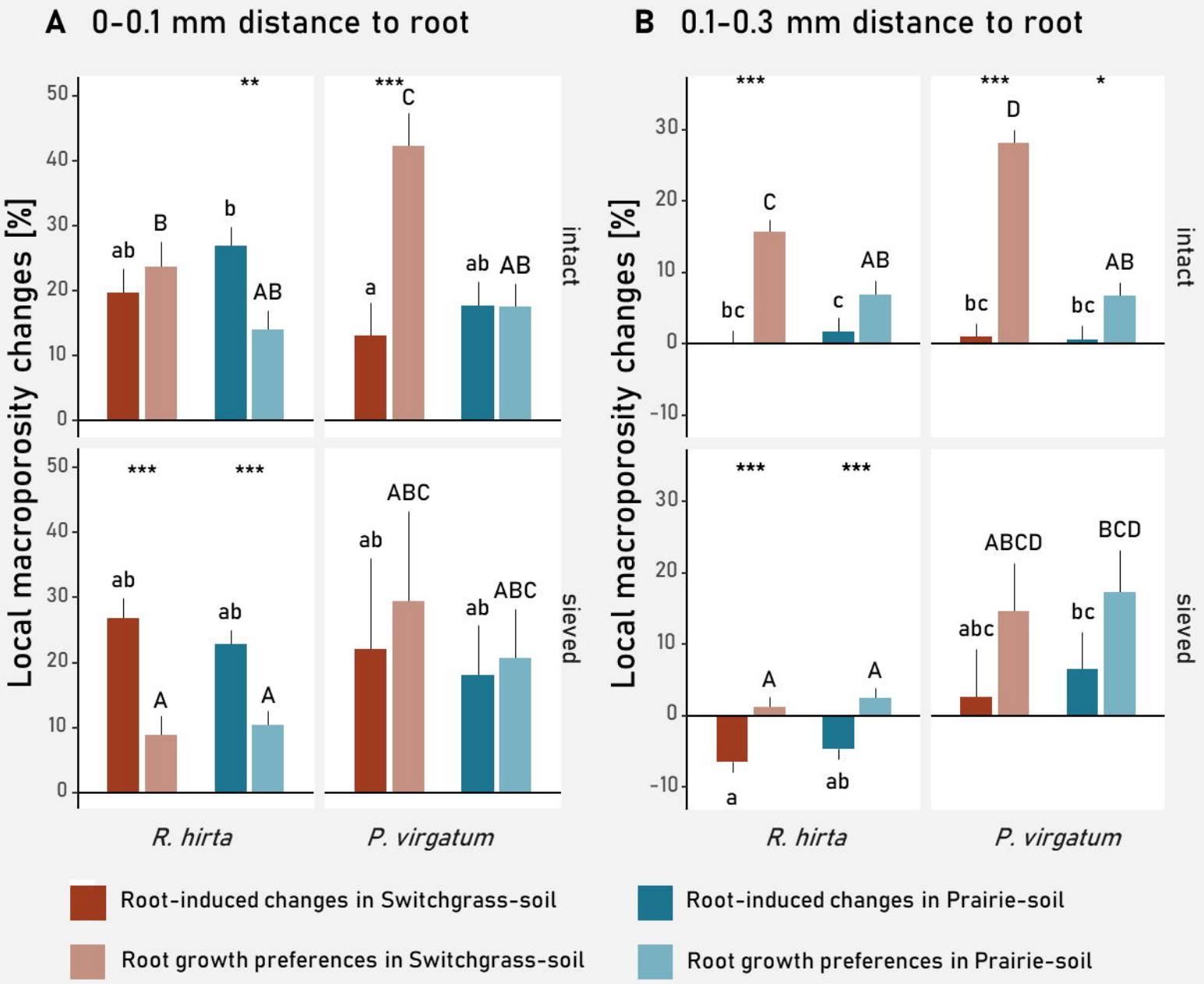
A 0-0.1 mm distance to root
B 0.1-0.3 mm distance to root
Local macroporosity changes [%]
intact
sieved
R. hirta
P. virgatum
Root-induced changes in Switchgrass-soil
Root growth preferences in Switchgrass-soil
Root-induced changes in Prairie-soil
Root growth preferences in Prairie-soil

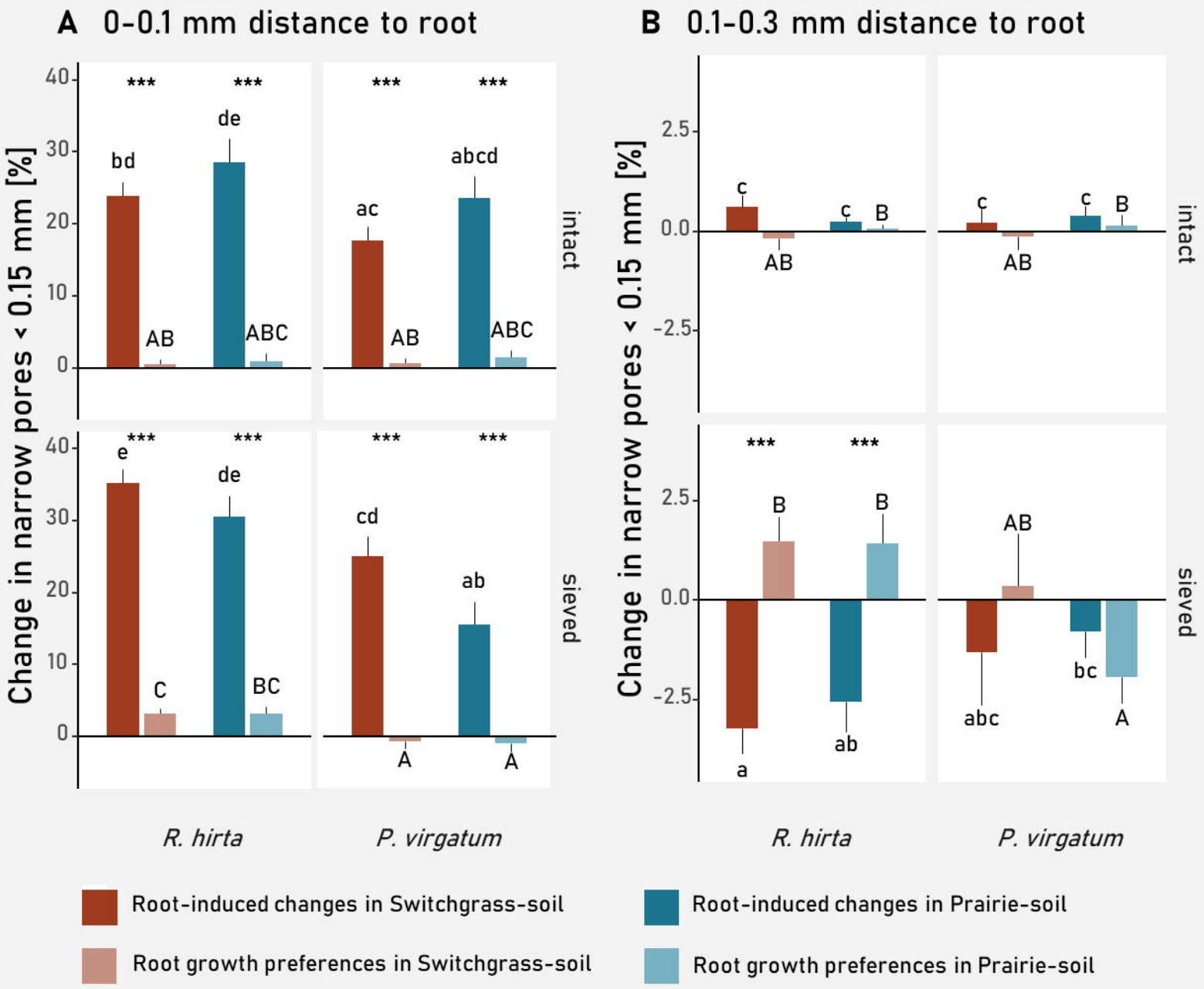
A 0-0.1 mm distance to root
B 0.1-0.3 mm distance to root
Change in narrow pores < 0.15 mm [%]
intact
sieved
R. hirta
P. virgatum
Root-induced changes in Switchgrass-soil
Root-induced changes in Prairie-soil
Root growth preferences in Switchgrass-soil
Root growth preferences in Prairie-soil

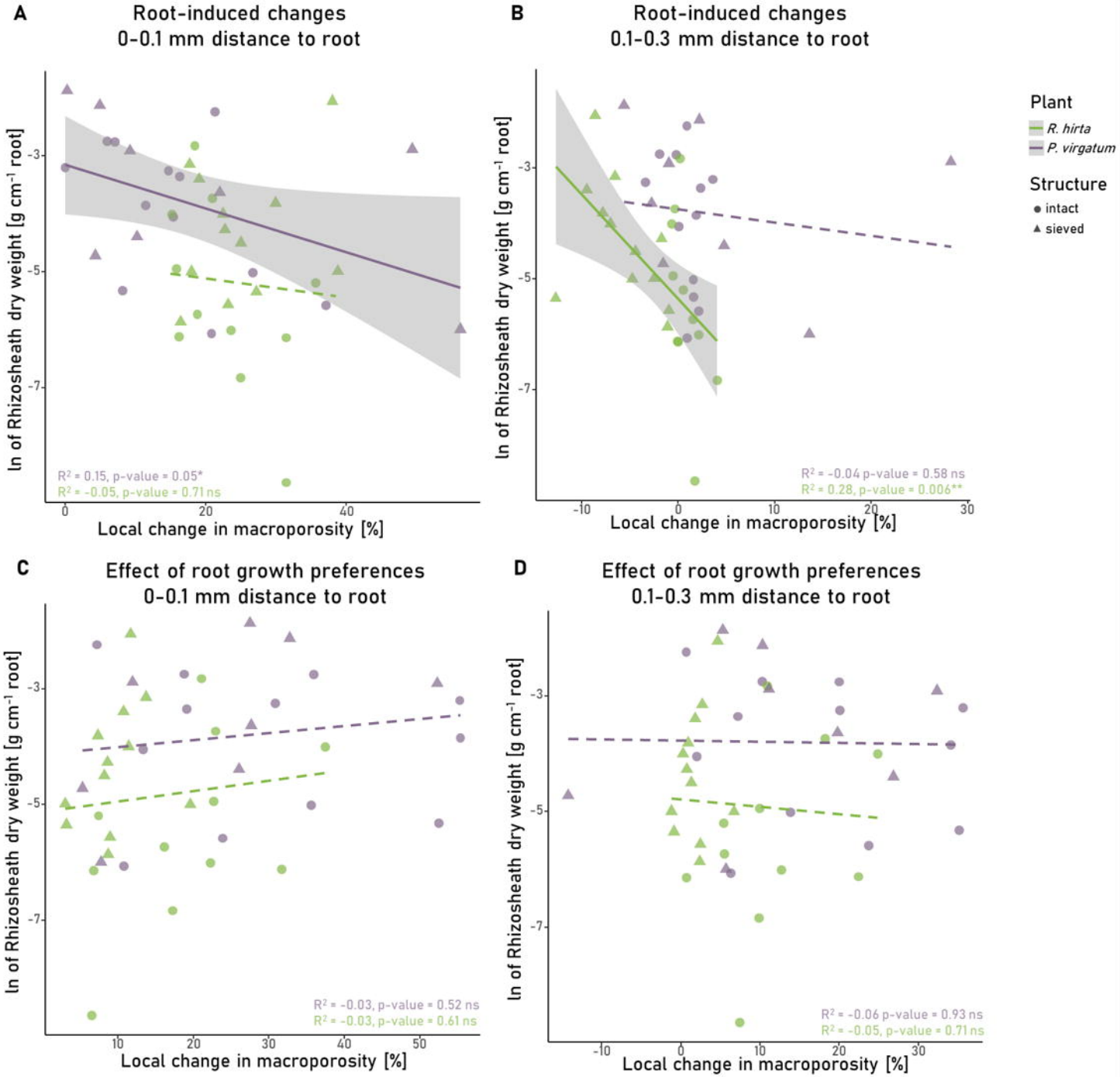
A
Root-induced changes
0-0.1 mm distance to root
B
Root-induced changes
0.1-0.3 mm distance to root
C
Effect of root growth preferences
0-0.1 mm distance to root
D
Effect of root growth preferences
0.1-0.3 mm distance to root
ln of Rhizosheath dry weight [g cm⁻¹ root]
Local change in macroporosity [%]
R² = 0.15, p-value = 0.05*
R² = -0.05, p-value = 0.71 ns
R² = -0.04 p-value = 0.58 ns
R² = 0.28, p-value = 0.006**
R² = -0.03, p-value = 0.52 ns
R² = -0.03, p-value = 0.61 ns
R² = -0.06 p-value = 0.93 ns
R² = -0.05, p-value = 0.71 ns
Plant
R. hirta
P. virgatum
Structure
intact
sieved